# SCIENTIFIC REPORTS

**OPEN**

# Markov modeling reveals novel intracellular modulation of the human TREK-2 selectivity filter

Matthew P. Harrigan [iD][1], Keri A. McKiernan [iD][1], Veerabahu Shanmugasundaram[2], Rajiah Aldrin Denny[3] & Vijay S. Pande[1,4,5,6]

Two-pore domain potassium (K2P) channel ion conductance is regulated by diverse stimuli that directly or indirectly gate the channel selectivity filter (SF). Recent crystal structures for the TREK-2 member of the K2P family reveal distinct "up" and "down" states assumed during activation via mechanical stretch. We performed 195 $\mu$s of all-atom, unbiased molecular dynamics simulations of the TREK-2 channel to probe how membrane stretch regulates the SF gate. Markov modeling reveals a novel "pinched" SF configuration that stretch activation rapidly destabilizes. Free-energy barrier heights calculated for critical steps in the conduction pathway indicate that this pinched state impairs ion conduction. Our simulations predict that this low-conductance state is accessed exclusively in the compressed, "down" conformation in which the intracellular helix arrangement allosterically pinches the SF. By explicitly relating structure to function, we contribute a critical piece of understanding to the evolving K2P puzzle.

TREK-2 is a member of the human K2P family of tandem-pore potassium channels. This protein is responsible for leak currents in nearly all cells. Its dysregulation has been linked to pain and depression, and it can be functionally regulated by mechanical stretch, heat, fatty acids, pH, secondary messengers of signaling proteins, and several drugs[1–3]. Recent evidence suggests that the regulatory processes acting on this channel modulate conductance through structurally distinct mechanisms[4]. However, the specific details of the conformational changes involved in these mechanisms remain unclear.

Potassium channel ion conductance is mediated by both an intracellular and interior gating process. The former involves large-scale rearrangements of the intracellular domains of the channel's transmembrane helices to sterically block passage of ions. Interior gating involves smaller conformational changes occurring directly in the channel's selectivity filter (SF), so named for its role in conferring potassium selectivity to the channel. The SF is formed by the p-loop domains connecting the protein subunits. These p-loops are arranged parallel to one another and are radially symmetric about the ion conduction pathway such that the backbone carbonyls point inward to form 4 adjacent binding sites (Fig. 1). Interior gating alters the stability of these binding sites.

In contrast to other types of potassium channels, switching of the TREK-2 intracellular gate is not thought to "close" the channel directly. Rather, the helical conformational changes confer information to the SF, which acts as the primary gate[5–7]. Recent crystal structures of TREK-2 provide structural insight into major conformational states involved in mechanical (stretch) activation by resolving distinct "up" (stretched) and "down" (compressed) conformations[8]. The number of bound ions observed for each state suggests differing levels of conductance, rather than closure of the channel. To understand how the channel switches between these conductance levels, we apply dynamical techniques to complement static crystal structures.

Molecular dynamics (MD) is a method for simulating biological systems with atom-level resolution. By using commodity GPUs[9] paired with a massively distributed architecture[10], simulations can reach biologically-relevant timescales. Advances in computing result in large quantities of high-dimensional time-series data. To draw

[1]Department of Chemistry, Stanford University, Stanford, CA, 94305, USA. [2]Medicinal Sciences, Pfizer Inc., Eastern Point Road, Groton, CT, 06340, USA. [3]Medicinal Sciences, Pfizer Inc., 610 Main Street, Cambridge, MA, 02139, USA. [4]Department of Computer Science, Stanford University, Stanford, CA, 94305, USA. [5]Department of Structural Biology, Stanford University, Stanford, CA, 94305, USA. [6]Program in Biophysics, Stanford University, Stanford, CA, 94305, USA. Matthew P. Harrigan and Keri A. McKiernan contributed equally to this work. Correspondence and requests for materials should be addressed to R.A.D. (email: Aldrin.Denny@pfizer.com) or V.S.P. (email: pande@stanford.edu)
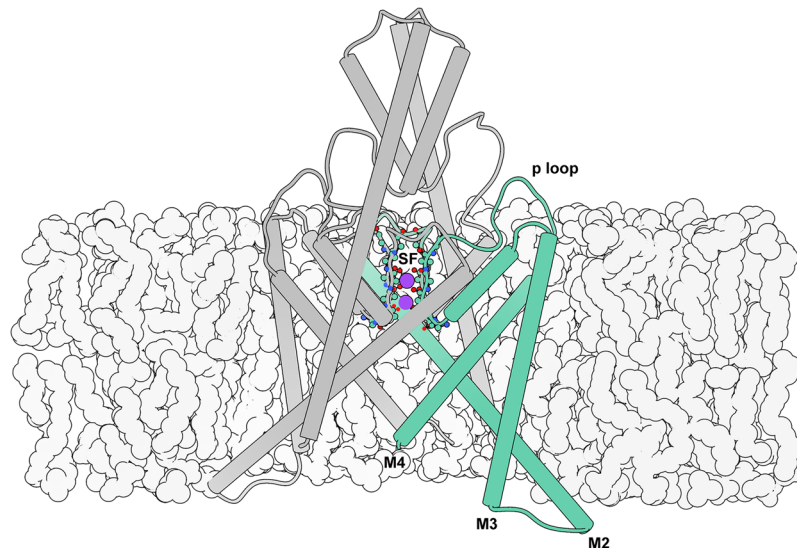
**Figure 1.** Illustration of the TREK-2 system. The selectivity filter (SF) is located at the center of the extracellular region of the membrane embedded pore, and is formed by the backbone of the four p loops. Here it is shown with occupancy corresponding to the simulated resting state. Intracellular gating involves movements of the M2, M3, and M4 helices, while interior gating involves conformational changes of the SF.

interpretable conclusions from this information, further analysis is required. Markov state models (MSMs) have gained favor for their robust, statistical analysis of biophysical systems[11–14]. Time-structure based independent component analysis (tICA) is a component of Markov state modeling that can aid in interpretability. tICA is a machine learning technique to find the slowly-decorrelating modes in high-dimensional time-series data. Biophysical processes of interest are often those that occur with the slowest timescales. By using tICA on a large set of input features, we avoid codifying our preconceived notions about the dynamics of the system into the analysis while still reducing the dimensionality of the system by projecting conformational features onto a small number ($\approx$5) of kinetically-motivated independent components (tICs). Finally, Potential of mean force (PMF) computations can complement MSM analysis by offering quantification of free-energy profiles along paths or coordinates of interest[15].

In this paper we investigate how the structural conformational changes involved in stretch activation influence the thermodynamics and kinetics of ion permeation. We sample along this pathway through unbiased MD simulation. We then examine the dynamical behavior of these simulations using Markov modeling. Specifically, we apply MSM analysis of the large MD dataset to survey equilibrium conformational dynamics. We detect a novel "pinched" configuration of the SF favored during compression. We survey SF equilibrium ion dynamics, and contrast structural macrostates' unique SF ion occupancy preferences. We compute PMF curves to quantitatively analyze the energetics involved in SF ion occupancy state transitions which show a correlation with both the whole-molecule and SF conformational states. Notably, the states favored under membrane compression have the most disfavored outward ion rectification. Our results predict a specific structural motif that we implicate in the coupling of intracellular and interior gates. We propose the novel conformation as a basis for future study.

## Results

**Dynamics of conformational change.** X-ray crystal structures offer an unrivaled atom-level view into static structures of proteins. The published crystal structures for TREK-2 identify two distinct stable conformations for the channel, presumed to be the result of membrane stretch and compression. The stretched, "up" state's transmembrane (M) helices are displaced upwards and outwards compared to the compressed, "down" state. The conformational differences are large compared to the size of the protein. In this paper, we refer to the states distinguished by large-scale motions as "macrostates". These static structures lack dynamical information, and the relative populations or free-energies of each macrostate in physiological conditions is unknown. We ran 195 μs of unbiased, explicit-solvent, explicit-membrane, isobaric molecular dynamics (MD) initialized with protein coordinates from the four crystal structures aiming to dynamically connect the experimentally observed structures and discover metastable or intermediate conformations inaccessible to crystallography.

Due to the large amount of data among many distributed trajectories, we apply state-of-the-art MSM modeling methods to glean insight from the large dataset. We use tICA to automatically discover an "up-down" stretch activation coordinate from a large number of atom-pair distances. Building an MSM on these coordinates permits generation of a 500 μs representative trajectory. By inspection, we identify the primary tIC as an "up-down" measurement. The up-down trace for the MSM trajectory is shown in Fig. 2A and a movie is available (see Fig. S1 and supporting files). The kinetic information in the MD dataset can be exploited to assign each observed conformation to a macrostate (Fig. 2B, contours). As a matter of notation, we refer to MSM-assigned macrostates corresponding to a specific ensemble of conformations with script-text (e.g. *Up*) to distinguish from abstract notions
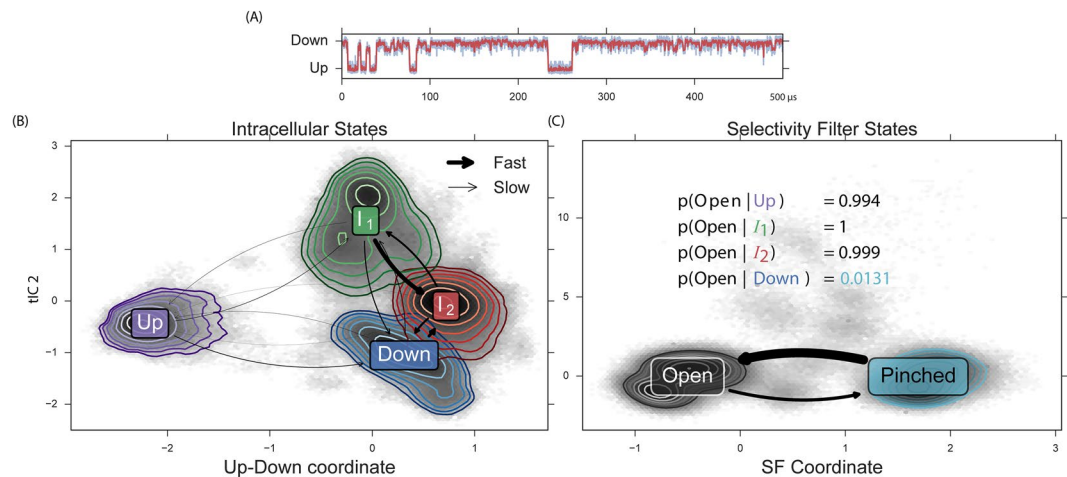
**Figure 2.** Automatic coordinate discovery using molecular dynamics data identifies an up-down coordinate from a set of high-dimensional input data. Modeling the observed dynamics by construction of an MSM permits rapid analysis of conformational dynamics. From our analysis, we discover a novel selectivity filter (SF) conformation. (**A**) MSM analysis permits generation of a $500\,\mu s$ representative trajectory which contains transitions between up, down, and intermediate conformations, see movie in SI. (**B**) We find four metastable conformational macrostates, shown as contours in tIC space. Transition rates show a rapid relaxation from $I_1$ to $I_2$, and a fast exchange between $I_2$ and *Down*. (**C**) Automatic coordinate discovery on the selectivity filter finds a structurally distinct pinched state. Inset enumerates the SF open probability as a function of intracellular macrostate. The *Up* and intermediate intracellular states favor an open SF, while the *Down* intracellular state strongly favors a pinched SF.

of states, which we quote (e.g. "up"). We investigate the kinetics and thermodynamics among the macrostates (Fig. 2B, arrows). We find a highly-populated *Down* state in exchange with an intermediate $I_2$, differing by a partial unfolding of the M2-M3 loop (Fig. S2). We find a metastable intermediate $I_1$ that rapidly relaxes to $I_2$ (Fig. S3). We find a kinetically-distant *Up* state that can transition to and from each of the other three states (Fig. 3A). The TREK-2 system is known to form fenestration sites between the membrane embedded helices wherein inhibitors may bind. The volume of these sites varies monotonically along the up-down coordinate (Fig. S4), with the largest corresponding to the *Down* states.

In addition to using tICA to discover an up-down coordinate, we focused the algorithm specifically on the selectivity filter region of the channel. Specifically, we use interatomic distances only among selectivity filter atoms as the input features to learn a second tICA model. In this case, the molecular dynamics reveals a metastable "pinched" conformation of the selectivity filter (Fig. 3B). This SF conformation is not represented in the TREK-2 crystal structures, and could describe a conformation similar to that assumed during C-type inactivation[16]. In this conformation, residues at the top of the $S_1$ binding site rotate outwards, away from the ion conduction pathway, while residues at the top of the $S_0$ binding site move inward. This inward movement is most drastic for G176 (A) and G176 (B) (where (A) signifies the protein chain), which restricts the pore from approximately 8.5 to 4.5 angstroms. We model the dynamics between two selectivity filter states (*Open* and *Pinched*) with a Markov model. The model suggests a free-energy minimum *Open* conformation and a metastable *Pinched* conformation (Fig. 2B). Comparing the structural macrostate and SF state for each conformation indicates that the *Pinched* SF conformation is strongly coupled to the channel's intracellular conformation. The *Pinched* SF state is more prevalent in the fully *Down* state by a ratio of 75:1 (Fig. 2C, inset table). In the *Up* and $I_2$ macrostates, the situation is reversed; the proportion of *Pinched* conformations observed is strongly disfavored and the *Open* configuration dominates. In the $I_1$ state, only the *Open* SF is seen. The disruption of symmetry and restriction in pore diameter caused by the rearrangements of upper-SF carbonyl oxygens in the *Pinched* state strongly suggests that this conformational difference will negatively affect ion conductance rates. In the following sections, we will provide evidence for this reduced conduction rate.

**Dynamics of selectivity filter ion occupancy.** TREK-2 not only exhibited large-scale conformational differences in the available crystal structures, but also subtle differences in ion binding. The "down" structures were crystallized with $3K^+$ while the "up" structure was crystallized with $4K^+$. Dong *et al.*[8] hypothesized that all four combinations of (up, down) $\times$ ($3K^+$, $4K^+$) states are accessible, despite only observing the two. By analogy to other channels, they hypothesized that $4K^+$ states are highly conductive and $3K^+$ states are less conductive.

We test these hypotheses with our MD dataset. Specifically, we investigate the effect of conformational macrostate on ion occupancy in the selectivity filter (SF). By first partitioning the data by conformational macrostate (*Up*, *Down*, $I_1$, and $I_2$), we construct four MSMs of ion dynamics to compare and contrast the observed ion microstates and rates (shown in Fig. 4A and C). Thick arrows represent rapid transitions. Figure 4A is the kinetic model for SF ion transitions in the *Up* conformation while Fig. 4C is for *Down* (see Figs S7 and 8 for $I_1$ and $I_2$).
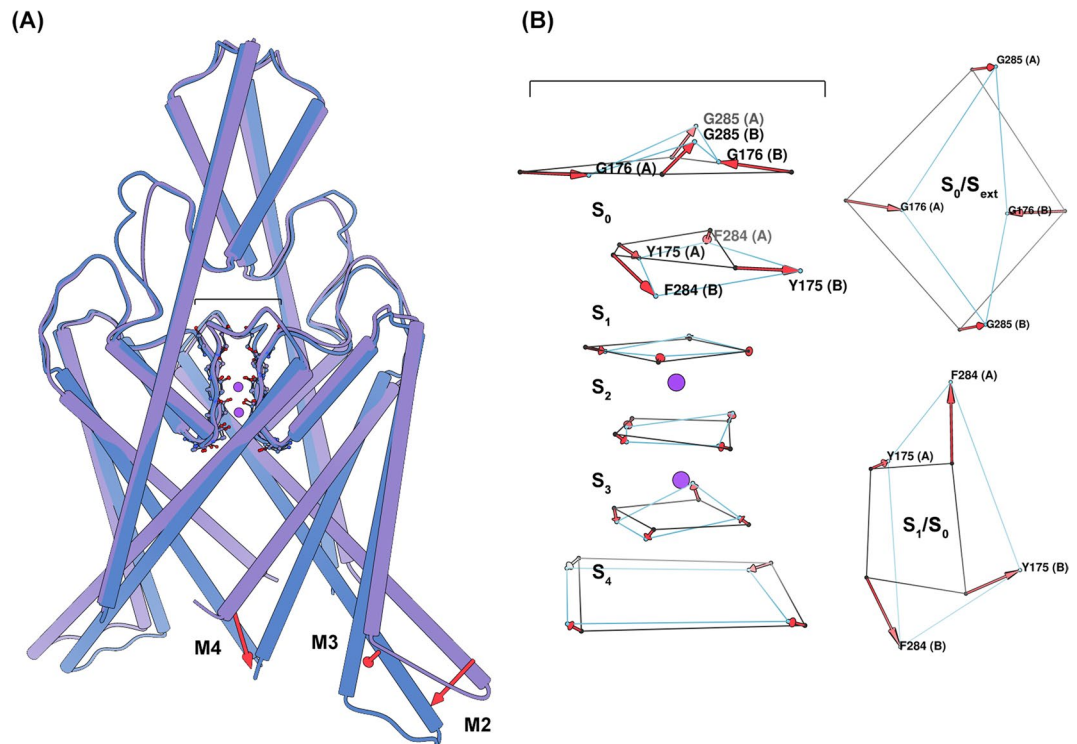
**Figure 3.** Conformational sampling of the MSM provides structural insight into the major states assumed during simulation. (**A**) A side-view of a superposition of the TREK-2 *Up* (purple) and *Down* (blue) intracellular macrostates, highlighting significant conformational differences. Transition from the *Up* to the *Down* state involves the large-scale inward movement of M2, M3, and M4. (**B**) A side-view (left) of a superposition of the TREK-2 SF *Open* (black) and *Pinched* (light blue) states, and aerial view (right) of the carbonyl oxygens at the interface of the $S_1/S_0$ and $S_0/S_{ext}$ binding sites. Here the SF is represented only by the carbonyl oxygens constituting the SF binding sites. Transition to the *Pinched* filter involves rotations of the residues surrounding the $S_1$ and $S_0$ binding sites. These changes disrupt the symmetry of the filter such that the $S_0/S_1$ carbonyls no longer face the ion conduction pathway (reducing the ability of these sites to coordinate ions), and the extracellular mouth of the filter is reduced in diameter by nearly 4 angstroms (G176 (A) - G176 (B)).

The relative populations of each ion microstate can be related to the up-down coordinate and is shown as a 2D-histogram in Fig. 4B.

Several trends are observed in these network graphs and population histogram. For all macrostates, OXXO [X = occupied; O = vacant; positions are given from $S_1$ to $S_4$ left-to-right] is found to be the dominant equilibrium ion microstate regardless of macrostate. The OXXO state serves as a sink with many observed transitions into it. This suggests that this state could represent the resting occupancy state. The higher ion occupancies observed in the crystal structures may be an artifact of the cryogenic crystallography conditions (investigated in ref. 17. In particular, Fig. S2 of its Supplementary Information). An additional commonality lies in the solvation of the SF ions. The hydration of the ions in the SF during the conduction process is an area of recent contention[18]. The soft knock-on mechanism posits that the ions are never directly adjacent, and they must be padded by at least one water molecule. The hard knock-on mechanism asserts that ions are preferably adjacent to one another. Both theories are based on the knock-on mechanism first formulated by Hodgkin and Keynes in 1955[19], wherein conduction is explained by the energetic perturbation of an ion entering the SF, and differ only with respect to ion solvation. We find that the full set of probable occupancy states determined from our simulations contains exclusively unsolvated ions. In fact, we observe very little water occupancy for any SF binding site, not just at the sites between ions, for all macroscopic conformations. We find the hard-knock mechanism described by Kopfer *et al.*[17] was supported by our simulations due to the degree of ion solvation and similarity between the set of most probable SF occupancy states. Note that TREK-2 is not canonically voltage sensing[20], so we would not expect the protein conformation to change drastically in the presence of a membrane potential.

The dissimilarities among the macrostate-specific MSMs are striking. The *Down* macrostate displays more diffuse ion dynamics with a large number of possible transitions among an extended state space. The equilibrium OXXO behaves less as a network sink with comparatively fewer high flux transitions into it. One might hypothesize that the greater ion movement would imply lower kinetic barriers and higher conduction. This is counter-intuitive as the down state has been suggested to be the low-conductivity state. While it is not clear how or to what extent the large, slow changes in macrostate impact the fast microstate transition pathways and stabilities, this joint conformation-ion analysis highlights qualitative differences that merit further study. To investigate quantitatively the effects of conformation on ion conduction, we perform additional simulation to study specific transitions in more detail.
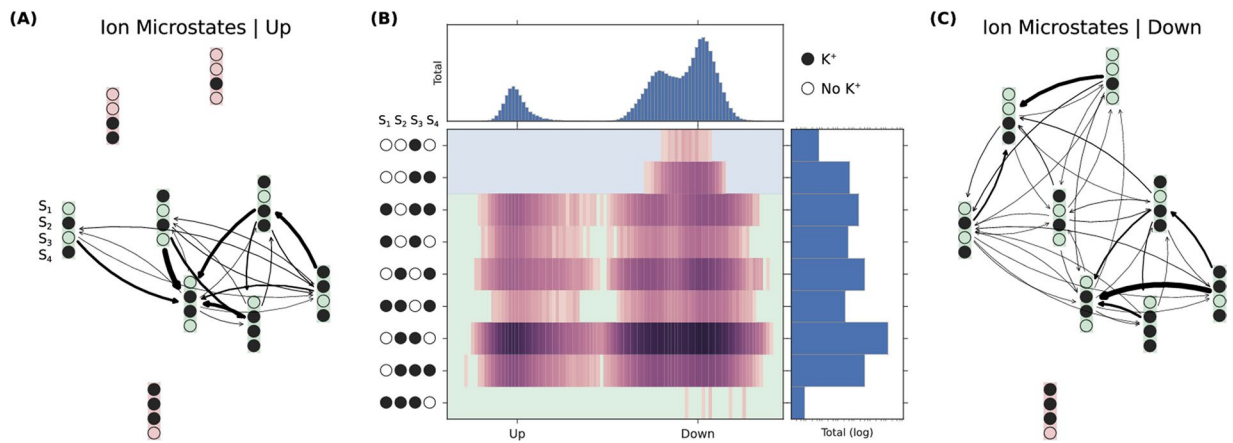
**Figure 4.** Ion conduction can be modeled as transitions among ion-occupancy states. (**A**) Transition rates between ion states in the *Up* macrostate conformation. (**B**) Populations of ion states as a function of the up-down coordinate identified by statistical analysis of the large-scale conformational dynamics. Relative free energies of the ion microstates are conformationally dependent. Additionally, some ion microstates are observed that exist solely in down conformations. (**C**) Transition rates between ion states in the *Down* macrostate conformations.

## Impact of structure on function.

Large-scale conformational changes among macrostates are suggested to impact the ion transition pathways in the selectivity filter, and therefore impact conduction. To quantify these differences, we partition the data by macrostate. For each macrostate, we compute PMF curves for key ion occupancy transitions. The OXXO → XXXO and XXOX → XOXX transitions were of particular interest because of their proposed role in the hard knock-on ion conduction mechanism.

The OXXO → XXXO transition describes the process of an ion moving from the intracellular channel cavity into the SF. This transition has been proposed to be most critical for the initiation of a conduction cycle. As can be seen in Fig. 5A left, the forward and reverse rates for this process are all less than 3 kCal mol$^{-1}$. The *Up* state is found to have the highest forward kinetic barrier, followed by the two intermediate states, with the *Down* states having the lowest. The reverse rates for each macrostate are comparable, but the sample from the conformation with the alternative SF conformation, *Down*$_{pinch}$ displays a highly destabilized second binding well.

The XXOX → XOXX transition describes the movement of an interior ion nearer to the SF exit, from $S_3$ to $S_2$. This transition was of interest because the conformations sampled from the MSM macrostates displayed variability in the structure of the SF on the extracellular side. This transition is closer to the region of SF structural variability. As shown by Fig. 5A right, the forward and reverse rates for this process are all less than 4 kCal mol$^{-1}$. The size of the forward barrier is highest for the Down states, followed by $I_2$, while $I_2$ and the up state are the lowest. Once again, the *Down*$_{pinch}$ sample yields a highly destabilized second binding well.

Although the *Down* state represents the least conductive state, for the OXXO → XXXO transition it displays the smallest forward kinetic barrier, and for the XXOX → XOXX transition it displays the largest forward kinetic barrier. This illustrates how the conductance rate can be understood only through the consideration of multiple transition events. Barriers are not uniformly higher for the *Down* state. Instead, the effect is stronger for our analyzed downstream conduction transition, especially in the case where an conformational change in the SF has occurred.

For both transitions, conformational macrostate is found to have a marked impact on the forward kinetic barriers, while SF conformation is found to have a marked impact on the reverse kinetic barriers. Alternative SF conformations are observed with the highest probability for the *Down* state from the MD dataset (see Fig. 2C and SI). The conformational changes associated with these alternative SF states are characterized by rotations of the backbone dihedral angles for the residues at the interface of the $S_1/S_0$ and $S_0/S_{ext}$ binding sites (see Fig. 3B). In the case that a backbone dihedral rotation did occur, the $S_1$ carbonyl oxygens no longer face the ion conduction pathway. Because the carbonyl oxygens of the residue backbone are responsible for coordinating the ions at each binding site, these rotations could render $S_1$ nonfunctional. Additionally, these rotations allow for the inward movement of the $S_0$ G176 (A) and G176 (B) residues. This movement appreciably restricts the diameter of the SF extracellular mouth, which could present a steric barrier to ion permeation.

Experimental studies show that TREK-2 exhibits a bidirectional allosteric coupling between the SF and the cytosolic proximal C-terminus[21], occurring via movements of M4. This coupling has been proven, but the exact conformational changes of the SF assumed during this process remain unknown. Similar movements of M4 occur during mechanical activation. It is therefore reasonable to propose that there exists an analogous allosteric coupling between the SF and the *Up* and *Down* states. However, because transitioning between the *Up* and *Down* states also involves movements of the M2 and M3 helices, we do not claim that this coupling is precisely the same. Markov modeling reveals the conformation of a *Pinched* SF filter that is starkly favored by the *Down* intracellular conformation, and PMF calculations demonstrate that the *pinched* SF disfavors extracellular ion rectification. We hypothesize that the intracellular rearrangements occurring as TREK-2 assumes the *Down* state transduces
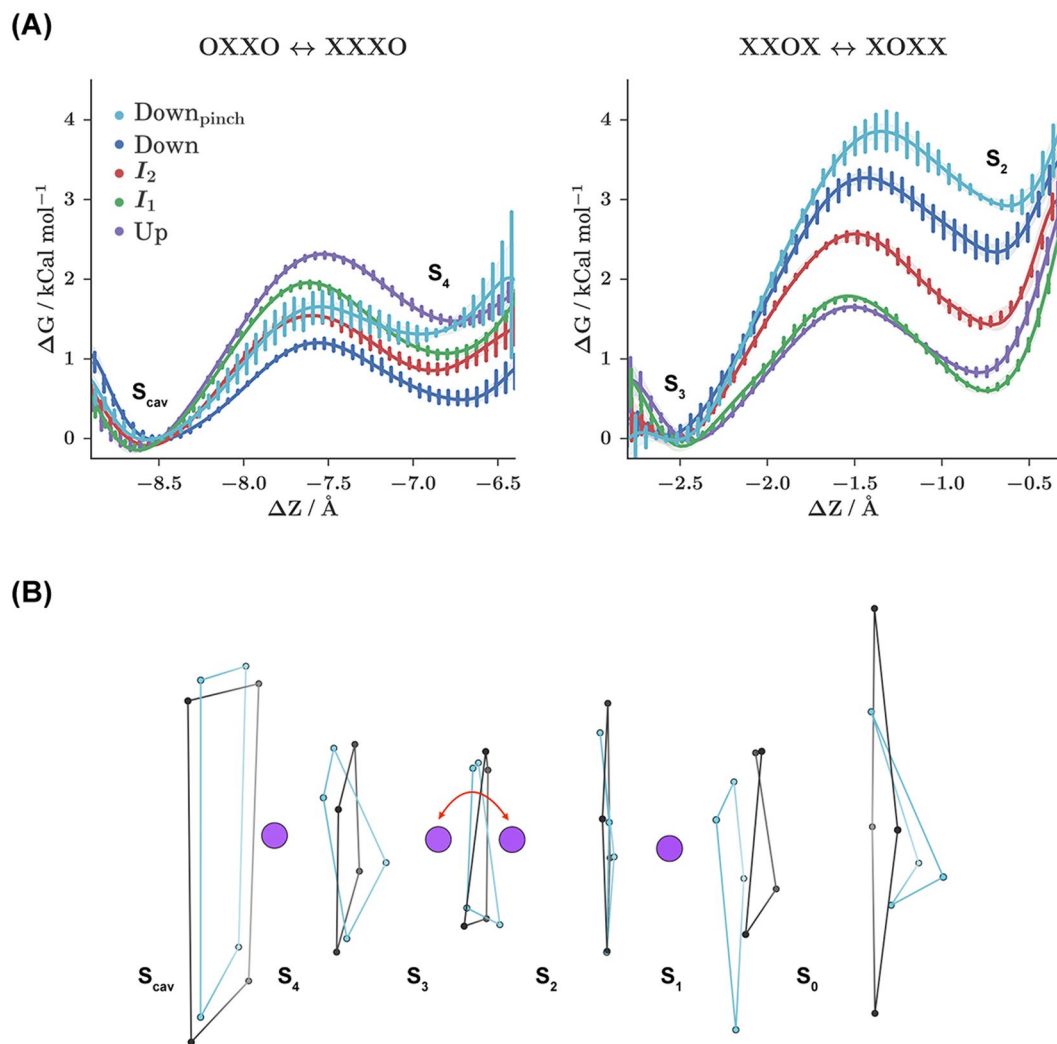
**(A)**



**(B)**



**Figure 5.** The energetics of ion occupancy transitions are conformationally dependent and can be analyzed using potential of mean force (PMF) calculations. For each conformational macrostate, PMF curves are computed for two key ion occupancy transitions. (**A**) Representative PMF curves for each macrostate. The *Down* macrostate favors the novel, pinched SF configuration and has been separated into *Down* (blue) and *Down*$_{pinch}$ (light blue) curves. $\Delta Z$ is progress along the ion transition path. (**B**) Illustration of the process sampled during the *XXOX* ↔ *XOXX* PMF calculations for the *Up*$_{Open}$ (black) and *Down*$_{pinch}$ SF states. This process represents the oscillation of an ion between the $S_3$ and $S_2$ binding sites, while occupancy of $S_4$ and $S_1$ remains static.

a conformational change of the SF residues at the interfaces of the $S_1/S_0$ and $S_0/S_{ext}$ ion binding sites, resulting in reduced ion conduction.

## Discussion

We applied molecular dynamics and MSM analysis to predict that a novel pinched state favored during membrane compression represents a low-conducting state of the TREK-2 K2P potassium channel. An initial hypothesis[8] suggested a direct connection between intracellular motion and channel activity. Membrane stretch and compression ("up" versus "down" macrostates) would beget high- and low-conducting functionality, respectively. This hypothesis has been suggested to be overly simplistic by experimental measurements[4] and the present study. After simulating the TREK-2 channel for 195 μs, we discover a novel selectivity filter conformation highly preferred by the *Down* state, but disfavored by the down-like $I_1$ and $I_2$ metastable intermediates and *Up* state. Steric consequences of this SF configuration suggest an impact on conductance. For further investigation, we use MSMs to model the behavior of ions in the selectivity filter conditioned on the conformational macrostate of the channel. Our ion dynamics models highlight similarities between the kinetic networks from the different conformations. In particular, the Kopfer[17] hard-knock mechanism is well supported by our simulations. The macrostate-conditioned models also suggest striking qualitative differences between ion microstate occupancies and transition paths. To gain a quantitative understanding of these differences, we selected representative conformations from our unbiased MD calculations and computed PMF free energy profiles for crucial ion transitions,

again partitioned by conformation. While the initial transition OXXO → XXXO shows the smallest barrier for down configurations (contrary to the idea that down conformations are less conductive), a later Köpfer pathway transition shows the highest barrier for down states, particularly the down state with pinched selectivity filter ($Down_{pinch}$). The $Down_{pinch}$ state is shown to have destabilized second wells in both important transitions studied, adding further evidence to the reduced activity of this conformation. Our findings agree with the growing consensus that intracellular motion is not directly coupled to conduction. Instead, conformational states affect selectivity filter conformations. We contribute a structural basis for this idea by the discovery of a novel pinched SF state involving rotations around Y175/F284. We encourage future structural studies to target this novel state.

## Methods

**Molecular Dynamics.** The simulations were started from four crystal structures of TREK-2 (PDB codes: 4xdj, 4bw5, 4xdl, 4xdk)[8] Crystal structures were solvated in a 4:1 POPC:POPE lipid bilayer membrane using charmm-gui[22]. Simulations inputs were generated using the tip3p[23], lipid14[24] and AMBER14SB[25] forcefields. Equilibration was performed with restrained proteins and lipids, by slowly increasing temperature from 0 K to 300 K in Amber 14[26]. The canonical forcefield was generated as a prmtop file using Amber's tLeap program. Production simulations were run at 300 K constant temperature and 1 bar constant pressure with constrained hydrogen bond lengths and rigid waters. Simulations were run on Folding@Home[10] using OpenMM 6.2[27] and Gromacs 4.5.3[28]. OpenMM simulations exploit GPUs while Gromacs is faster for CPUs, and the two codes were used simultaneously. Production simulations used a 2.0 fs timestep and the particle mesh Ewald (PME) method for electrostatics. There is not a consistent choice of thermostat and barostat implemented in these two codes. Rather, we used the recommended NPT settings for each code. OpenMM simulations used a Langevin integrator with a 1.0/ps friction coefficient and a (fully) anisotropic Monte Carlo barostat with a frequency of 25 steps. OpenMM natively reads the prepared forcefield prmtop files. For Gromacs, ParmEd (https://github.com/ParmEd/ParmEd) was used to convert the prmtop topology to the Gromacs "top" format. Gromacs simulations used the velocity-rescaling-with-stochastic-term temperature coupling with a time constant of 2.0 ps and a Parrinello-Rahman barostat with time constant of 2.0 ps.

PMF calculations were run with Gromacs 5.0.5 on Bluewaters and reweighted with WHAM[29]. Analysis was performed with MDTraj 1.5[30] and MSMBuilder 3.4[31]. Conformations were visualized with VMD[32] and Chimera[33].

**Markov State Modeling.** The pore region of the protein was featurized by taking all respective chain A to chain B distances between residues 1–24, 112–189, 230–256. These features were transformed into kinetic coordinates with tICA (lag-time = 1 ns). Conformations were clustered into 500 states using the first 3 dimensions of tIC coordinates via the Mini-batch KMeans algorithm. An MSM was fit using MLE at a lag-time of 20 ns. Conformational microstates were lumped into four macrostates with PCCA+. Ion occupancies were featurized by enumerating the 16 possible occupancy states (from four binding sites). An MSM was fit using MLE, again at a lag-time of 20 ns.

**PMF Calculations.** PMF initial conformations were obtained through PCA analysis on the protein dihedral angles for each MSM state. These conformations were aligned such that the SF was centered about the z-axis. Pulling simulations were performed in order to sampling the reaction coordinate for each ion transition. Five umbrella sampling simulations were run for each PMF, one in each ion binding well, one at the transition state, and one between each binding well and the transition state. This arrangement resulted in a window spacing of approximately 0.05 nm. These simulations were run with a spring constant of 8000 kCal mol$^{-1}$ for 6 ns, with the first 1 ns treated as equilibration. Convergence was determined by monitoring the overlap between simulation histograms. For each transition and macrostate, at least 8 conformations were analyzed. PMF error bars were computed over these conformations. The PMF reaction coordinate was defined as the projection of the distance from the SF center of mass to the transitioning ion onto the SF symmetric axis. All PMF related simulations were run using Gromacs 5.0.5[28]. RMSD of protein conformation to initial structure was monitored during umbrella sampling simulations to ensure there were no artifacts caused by the umbrella potential.

## References

1. Enyedi, P. & Czirjak, G. Molecular background of leak k+ currents: Two-pore domain potassium channels. *Physiological Reviews* **90**, 559–605 (2010).
2. Lesage, F., Terrenoire, C., Romey, G. & Lazdunski, M. Human trek2, a 2p domain mechano-sensitive k+ channel with multiple regulations by polyunsaturated fatty acids, lysophospholipids, and gs, gi, and gq protein-coupled receptors. *Journal of Biological Chemistry* **275**, 28398–28405 (2000).
3. Noël, J., Sandoz, G. & Lesage, F. Molecular regulations governing trek and traak channel functions. *Channels* **5**, 402–409 (2011).
4. McClenaghan, C. *et al.* Polymodal activation of the trek-2 k2p channel produces structurally distinct open states. *The Journal of general physiology* **147**, 497–505 (2016).
5. Goldstein, S. A., Bockenhauer, D., O'Kelly, I. & Zilberberg, N. Potassium leak channels and the kcnk family of two-p-domain subunits. *Nature Reviews Neuroscience* **2**, 175–184 (2001).
6. Piechotta, P. L. *et al.* The pore structure and gating mechanism of k2p channels. *The EMBO journal* **30**, 3607–3619 (2011).
7. Rapedius, M. *et al.* State-independent intracellular access of quaternary ammonium blockers to the pore of trek-1. *Channels* **6**, 473–478 (2012).
8. Dong, Y. Y. *et al.* K2p channel gating mechanisms revealed by structures of TREK-2 and a complex with prozac. *Science* **347**, 1256–1259 (2015).
9. Friedrichs, M. S. *et al.* Accelerating molecular dynamic simulation on graphics processing units. *J. Comput. Chem.* **30**, 864–872 (2009).
10. Shirts, M. & Pande, V. S. Screen savers of the world unite! *Science* **290**, 1903–1904 (2000).
11. Pande, V. S., Beauchamp, K. & Bowman, G. R. Everything you wanted to know about markov state models but were afraid to ask. *Methods* **52**, 99–105 (2010).
12. Schwantes, C. R., McGibbon, R. T. & Pande, V. S. Perspective: Markov models for long-timescale biomolecular dynamics. *J. Chem. Phys.* **141**, 090901 (2014).

13. Chodera, J. D. & Noé, F. Markov state models of biomolecular conformational dynamics. *Curr. Opin. Struct. Biol.* **25**, 135–144 (2014).
14. Bowman, G. R., Pande, V. S. & Noé, F. *An Introduction to Markov State Models and Their Application to Long Timescale Molecular Simulation*, vol. 797 (Springer, 2014).
15. Park, S. & Schulten, K. Calculating potentials of mean force from steered molecular dynamics simulations. *The Journal of Chemical Physics* **120**, 5946 (2004).
16. Hoshi, T., Zagotta, W. N. & Aldrich, R. W. Two types of inactivation in shaker k+ channels: effects of alterations in the carboxy-terminal region. *Neuron* **7**, 547–556 (1991).
17. Kopfer, D. A. *et al.* Ion permeation in k+ channels occurs by direct coulomb knock-on. *Science* **346**, 352–355 (2014).
18. Hummer, G. Potassium ions line up. *Science* **346**, 303–303 (2014).
19. Hodgkin, A. L. & Keynes, R. The potassium permeability of a giant nerve fibre. *The Journal of Physiology* **128**, 61–88 (1955).
20. Schewe, M. *et al.* A non-canonical voltage-sensing mechanism controls gating in k2p k+ channels. *Cell* **164**, 937–949 (2016).
21. Ren-Gong Zhuo, P. P. *et al.* Allosteric coupling between proximal c-terminus and selectivity filter is facilitated by the movement of transmembrane segment 4 in trek-2 channel. *Scientific reports* **6** (2016).
22. Lee, J. *et al.* CHARMM-GUI input generator for NAMD, GROMACS, AMBER, OpenMM, and CHARMM/OpenMM simulations using the CHARMM36 additive force field. *J. Chem. Theory Comput.* **12**, 405–413 (2016).
23. Jorgensen, W. L., Chandrasekhar, J., Madura, J. D., Impey, R. W. & Klein, M. L. Comparison of simple potential functions for simulating liquid water. *The Journal of chemical physics* **79**, 926–935 (1983).
24. Dickson, C. J. *et al.* Lipid14: The amber lipid force field. *J. Chem. Theory Comput.* **10**, 865–879 (2014).
25. Maier, J. A. *et al.* ff14sb: improving the accuracy of protein side chain and backbone parameters from ff99sb. *Journal of chemical theory and computation* **11**, 3696–3713 (2015).
26. Case, D. A., Babin, V., Berryman, J. T., Betz, R. M., Cai, Q., Cerutti, D. S., Cheatham, T. E. III, Darden, T. A., Duke, R. E., Gohlke, H. Goetz, A. W., Gusarov, S., Homeyer, N., Janowski, P., Kaus, J., Kolossváry, I., Kovalenko, A., Lee, T.S., LeGrand, S., Luchko, T., Luo, R. Madej, B., Merz, K. M., Paesani, F., Roe, D.R., Roitberg, A., Sagui, C., Salomon-Ferrer, R., Seabra, G., Simmerling, C. L., Smith, W., Swails, J., Walker, R. C., Wang, J., Wolf, R. M., Wu, X. & Kollman P. A. University of California, San Francisco *Amber* 14 (2014).
27. Eastman, P. *et al.* Openmm 4: A reusable, extensible, hardware independent library for high performance molecular simulation. *Journal of Chemical Theory and Computation* **9**, 461–469 (2013).
28. Abraham, M. J. *et al.* GROMACS: High performance molecular simulations through multi-level parallelism from laptops to supercomputers. *SoftwareX* **1–2**, 19–25 (2015).
29. Kumar, S., Rosenberg, J. M., Bouzida, D., Swendsen, R. H. & Kollman, P. A. THE weighted histogram analysis method for free-energy calculations on biomolecules. i. the method. *J. Comput. Chem.* **13**, 1011–1021 (1992).
30. McGibbon, R. T. *et al.* MDTraj: A modern open library for the analysis of molecular dynamics trajectories. *Biophysical Journal* **109**, 1528–1532 (2015).
31. McGibbon, R. T. *et al.* msmbuilder: Msmbuilder 3.4. URL http://dx.doi.org/10.5281/zenodo.48545 (2016).
32. Humphrey, W., Dalke, A. & Schulten, K. VMD - Visual Molecular Dynamics. *Journal of Molecular Graphics* **14**, 33–38 (1996).
33. Pettersen, E. F. *et al.* Ucsf chimeraa visualization system for exploratory research and analysis. *Journal of computational chemistry* **25**, 1605–1612 (2004).

## Acknowledgements

## Author Contributions

All authors designed the research. M.P.H. and K.A.M. performed the research. R.A.D. and V.S.P. supervised the research. All authors edited and approved the manuscript.

## Additional Information

**Supplementary information** accompanies this paper at doi:10.1038/s41598-017-00256-y

**Competing Interests:** The authors declare that they have no competing interests.

**Publisher's note:** Springer Nature remains neutral with regard to jurisdictional claims in published maps and institutional affiliations.